Journal of GeoEngineering, Vol. 10, No. 3, pp. 83-89, December 2015
http://dx.doi.org/10.6310/jog.2015.10(3).2

PREDICTING PERIODIC RAINFALL-INDUCED SLOPE DISPLACEMENTS USING FORCE-EQUILIBRIUM-BASED FINITE DISPLACEMENT METHOD

Ching-Chuan Huang[1*] and Shan-Wun Yeh[2]

ABSTRACT

A cost- and time-effective derivation of the strength parameters for deep-seated sliding surfaces in natural slopes consisting of highly weathered or fractured rocks is of high practical importance. A force-equilibrium-based finite displacement method (FFDM) is used to back-calculate material property to alleviate possible difficulties in evaluating strength and deformation properties of highly weathered rocks using undisturbed soil sampling for a deep-seated sliding surface. The FFDM incorporates Bishop's slice method and nonlinear shear stress-displacement relationships. As a result, shear displacements along a circular potential failure surface can be computed. The displacement-related parameters obtained from a back-analysis using FFDM are then used to predict long-term cumulative slope displacements induced by periodic ground water table fluctuations. Results of the analytical study show that the long-term cumulative slope displacement of the slope can be well-predicted using the displacement-related parameters back-calculated from the first event of slope displacement induced by a groundwater table rise.

Key words: Rainfall-induced slope displacement, force equilibrium, case study, slice method, finite displacement method, hyperbolic soil model.

1. INTRODUCTION

Conventional slope stability methods are based on the principle of limit equilibrium (or force equilibrium), providing a single value of safety factor (F_s) for the analyzed slope without displacement-related output. On the other hand, the finite element method (FEM) has been used to provide information of slope displacements (Ho 2014). However, to perform a reliable FEM analysis often requires additional costs and time for personnel training, computer time, material testing, and output evaluation by an experienced advisor. It is apparent that a gap exists between a conventional limit-equilibrium-based slope stability analysis and a FEM analysis. To bridge this gap, a force-equilibrium-based finite displacement method (FFDM) was developed to achieve a time- and cost-efficient slope displacement calculation (Huang 2013; 2014; Huang *et al.* 2014). Other than the principles of force and moment equilibrium as used in the method of slices (*e.g.*, Fellenius 1936; Bishop 1955, Janbu 1973), the FFDM incorporates: (1) a hyperbolic shear stress vs. shear displacement model based on the results of large-scale direct shear tests; (2) a straightforward closed-form solution for the slope displacement; (3) an incremental displacement induced by the differential stress states of the slope. A well-monitored slope (the Ru-San slope) with a known surface of sliding and measured slope displacements is focused here to examine the applicability of circular failure surfaces and associated force-equilibrium formula.

2. BISHOP'S SLICE METHOD

Based on the force equilibrium in the vertical direction and the moment equilibrium about the center of rotation, Bishop (1955) derived the following equation for the safety factor (F_s) of slopes subjected to circular failure mechanism (Fig. 1):

$$F_s = \frac{\sum\left[C_i + (W_i - U_i \cos\alpha_i)\cdot\tan\phi\cdot\sec\alpha_i\right] \Big/ \left(1 + \dfrac{\tan\alpha_i\cdot\tan\phi}{F_s}\right)}{\sum(W_i\cdot\sin\alpha_i)} \tag{1}$$

$$C_i = c\cdot\ell_i = c\cdot B_i\cdot\sec\alpha_i \tag{2}$$

$$U_i = u_i\cdot\ell_i = u_i\cdot B_i\cdot\sec\alpha_i \tag{3}$$

where

i : slice number ($i = 1, 2, \ldots, ns$)
W_i : self-weight of slice i
α_i : inclination angle of slice base i
c : cohesion intercept of soil
ϕ : internal friction angle of soil
u_i : pore water pressure acting at the base of slice i
ℓ_i, B_i : the length of the base and the width, respectively, for slice i.

3. FORCE-EQUILIBRIUM-BASED FINITE DISPLACEMENT METHOD (FFDM)

For a sliced potential failure mass confined by a slip surface with a circular failure surface (as shown in Fig. 1), a local stress-based safety factor, FS_i, is defined as:

Manuscript received July 16, 2015; revised September 4, 2015; accepted October 7, 2015.

[1] Professor (corresponding author), Department of Civil Engineering, National Cheng Kung University, Tainan, Taiwan 70101 (e-mail: samhcc@mail.ncku.edu.tw).

[2] Graduate student, Department of Civil Engineering, National Cheng Kung University, Tainan, Taiwan, 70101 (e-mail: N66014297@ncku.edu.tw).

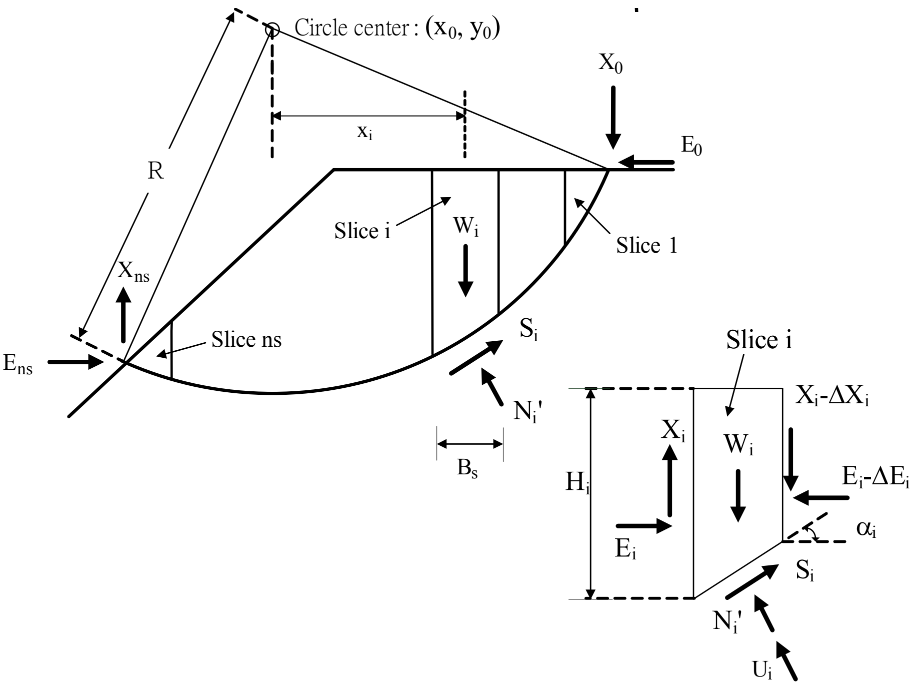

Fig. 1 Forces acting on the slice of a circular failure mass

$$FS_i = \frac{\tau_{f_i}}{\tau_i} = \frac{S_{fi}}{S_i} \tag{4}$$

where

τ_{fi} : failure shear stress at the base of slice i

τ_i : shear stress at the base of slice i

S_i : shear force at the base of slice i (= $\tau_i \times l_i$)

S_{fi} : failure shear strength at the base of slice i (= $\tau_{fi} \times l_i$)

A non-linear shear stress (τ_i) vs. shear displacement (Δ_i) relationship at the base of slice i is expressed using hyperbolic functions (Fig. 2):

$$\tau_i = \frac{\Delta_i}{a + b \cdot \Delta_i} \tag{5}$$

where

$$a = \frac{1}{k_{initial}} \tag{6}$$

$$b = \frac{R_f}{\tau_{fi}} \tag{7}$$

$k_{initial}$: initial stiffness of the stress-displacement curve

R_f : ratio between the failure stress and the ultimate asymptote stress

Mohr-Coulomb's failure criterion is valid for the soil strength at the base of slice i:

$$\tau_{fi} = c + \sigma'_{n_i} \cdot \tan\phi \tag{8}$$

where

σ'_{n_i} : effective normal stress acting on the base of slice i

τ_{fi} : shear strength of soil at the base of slice i (= S_{fi} / l_i)

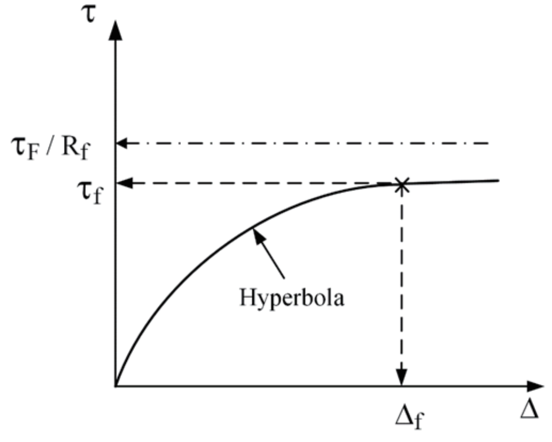

Fig. 2 Schematic figure of hyperbolic shear stress vs. shear displacement relationship

$$S_{fi} = \left[C_i + (W_i - U_i \cos\alpha_i) \cdot \tan\phi \cdot \sec\alpha_i\right] \Big/ \left(1 + \frac{\tan\alpha_i \cdot \tan\phi}{FS_i}\right) \tag{9}$$

It is assumed that the initial shear modulus ($k_{initial}$) of the stress-displacement curve is an exponential function of effective normal pressure on the failure surface (or slice base), σ'_n, which is similar to that used in evaluating the Young's modulus ($E_{initial}$) of soils:

$$k_{initial} = K \cdot G \cdot \left(\frac{\sigma'_{n_i}}{P_a}\right)^n \tag{10}$$

where

K : initial shear stiffness number

n : exponent for the initial shear stiffness function

G : reference shear stiffness (= 101.3 kPa/m)

P_a : atmospheric pressure (= 101.3 kPa)

Based on comprehensive studies on the shear stress-displacement relationships conducted by Huang (2013, 2014), Huang *et al*. (2014(a), (b)) and Yeh (2015), behavior of various undisturbed and remolded soils can be described using the hyperbolic model expressed by Eqs. (5) ~ (10). Results also indicate that three soil constants used in the hyperbolic model, namely K, n, and R_f, are in the range of: $K = 100 \sim 1000$; $n = 0.03 \sim 0.4$; $R_f = 0.6 \sim 0.97$.

Shear displacement at the base of slice i (Δ_i), can be related to the vertical displacement at slope crest, Δ_o, (Fig. 3) based on kinetic compatibility requirement (or hodogram; *e.g.*, Atkinson 1981) as:

$$\Delta_i = \Delta_o \cdot f(\alpha_i) \tag{11}$$

$$f(\alpha_i) = \frac{1}{\sin(\alpha_1 - \psi)} \cdot \frac{\cos(\alpha_1 - 2\psi)}{\cos(2\psi - \alpha_i)} \tag{12}$$

where

ψ : dilatancy angle ($\psi = 0$ is assumed in the following analyses)

Figure 4 shows an example of the displacement compatibility function, $f(\alpha_i)$ for the potential failure surface of the Ru-San slope (Fig. 6). It can be seen that trends for the cases of $\psi = 0$ and $\psi = \phi/2$ are different; the former case demonstrates a gradual decreasing trend towards the slope toe; the latter case shows a concave-upward shape. In the present study, the case of $\psi = 0$ is used because the slope is undergoing a measurable cumulative displacement.

4. FFDM USING CIRCULAR FAILURE SURFACES

Huang *et al*. (2014(a)) incorporated Bishop's slice method with additional kinetic requirements (Eqs. (11) ~ (12)) and hyperbolic shear stress-displacement constitutive laws (Eqs. (4) ~ (10)) to derive a closed form solution for Δ_0 as:

$$\Delta_0 = \frac{\sum(W_i \cdot \sin\alpha_i)}{\sum\left[\dfrac{f(\alpha_i)}{a + b\cdot f(\alpha_i)}\right]\cdot\left\{\left[C_i + (W_i - U_i\cdot\cos\alpha_i)\tan\phi\cdot\sec\alpha_i\right] / \left[1 + \dfrac{\tan\alpha_i\cdot\tan\phi\cdot\Delta_0\cdot f(\alpha_i)}{a + b\cdot\Delta_0\cdot f(\alpha_i)}\right]\right\}} \tag{13}$$

Comparing Eqs. (1) and (13), it can be seen that Eq. (13) is basically a reversed form of Eq. (1), with additional displacement-related terms such as a, b, $f(\alpha_i)$, and Δ_0. It is also noted that Eq. (13) is a nonlinear one (with the unknown Δ_0 exists in both sides). It takes several iterative calculations to obtain a converged value of Δ_0. This is also true for the case of calculating a converged value of F_s using Eq. (1).

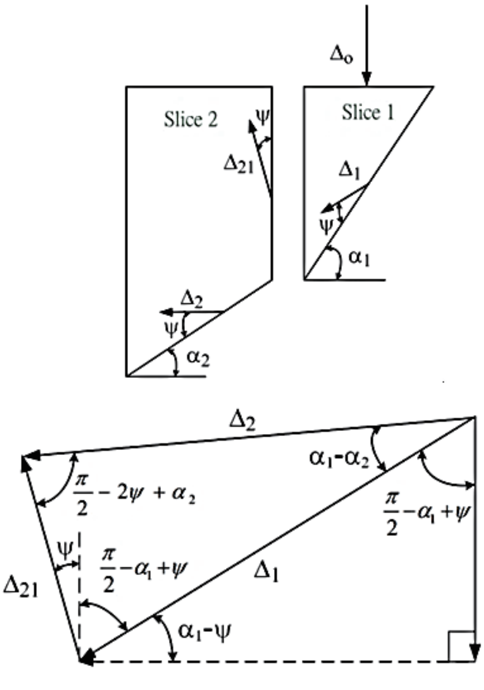

Fig. 3 Schematic figure of kinetic compatibility

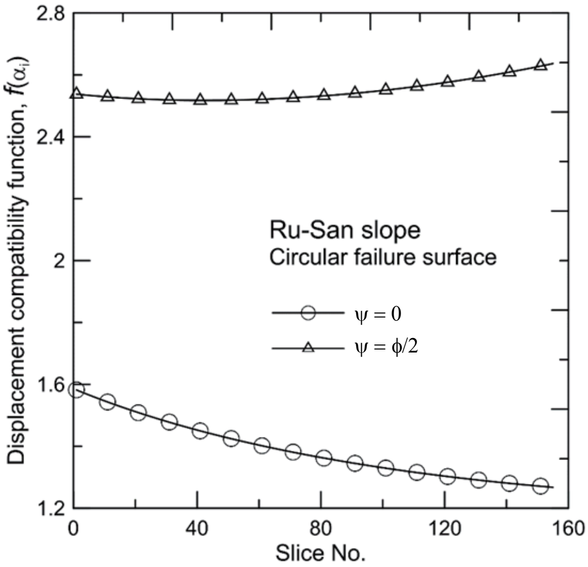

Fig. 4 Displacement compatibility function $f(\alpha_i)$ for the potential failure surface focused in the present study

5. INCREMENTAL SLOPE DISPLACEMENTS

An incremental slope displacement induced by a rainfall-induced groundwater table rise (Δ_i^{incr}) is expressed as the deviation between the post-rainfall displacement state (Δ_i^b) and the pre-rainfall displacement state (Δ_i^a), *i.e.*,

$$\Delta_i^{incr} = \Delta_i^b - \Delta_i^a \tag{14}$$

A personal computer program (SLICE-DISP) is used to compute values of Δ_i^{incr} induced by groundwater table rises during a period of slope displacement and groundwater table monitoring. SLICE-DISP is coded with BASIC-language on the platform of Visual Studio Community 2013 (Microsoft 2013). The computational flow can be summarized as follows:

1. Input data (slip surface coordinates; slope surface coordinates; soil strength parameters: c, ϕ; hyperbolic stress-displacement parameters: K, n, R_f).
2. Perform a conventional constant-F_s analysis using Bishop's method to obtain a conventional value of F_s using Eq. (1).
3. Calculate values of S_{fi} and σ'_{n_i} ($i = 1, \ldots, ns$) using Eqs. (9) and (8), respectively. For the 1st round computation, use $FS_i = F_s$ ($i = 1, \ldots, ns$) obtained in step (2), otherwise use updated values of FS_i.
4. Calculate values of a, b, and $f(\alpha_i)$ using Eqs. (6), (7), and (12), respectively.
5. Calculate Δ_0 and Δ_i using Eqs. (13) and (11), respectively.
6. Calculate τ_i ($i = 1, \ldots, ns$), using Eq. (5).
7. Calculate local safety factors, FS_i ($i = 1, \ldots, ns$), using Eq. (4).
8. Update values of a, b and $f(\alpha_i)$ using updated values of σ'_{n_i} and S_{fi}.
9. Calculate Δ_0 and Δ_i ($i = 1, \ldots, ns$) using Eqs. (13) and (11).
10. Check the convergence of Δ_0 based on the following criterion (Iterate from step (3) if not satisfied):

    $$\frac{(\Delta_0)_{new} - (\Delta_0)_{old}}{(\Delta_0)_{new}} \le \varepsilon \tag{15}$$

    where

    ε : convergence criterion ($\varepsilon = 1\%$ in the present study).
11. Calculate final values of FS_i and Δ_i ($i = 1, \ldots, ns$), using Eqs. (4) and (11), respectively.
12. Calculate pre- and post-rainfall slope displacements, Δ_i^a and Δ_i^b, based on pre- and post-rainfall groundwater tables, respectively, using steps (1) ~ (11).
13. Calculate rainfall-induced slope displacements (Δ_i^{incr}) using Eq. (14).

6. CASE STUDY ON RU-SAN SLOPE

Figure 5 shows the location of the studied slope (the Ru-San slope) which is a part of Route No. 14 winding through a tectonically active region where the epicenter of the 1999 Chi-Chi earthquake ($M_L = 7.3$; M_L: Richter scale for earthquake) was located. The sliding mass spans over an area of 30 ha. (820 m-long, max. 480 m-wide). Figure 6 shows the cross section A-A' of the Ru-San slope with a deep-seated slip surface approximately along the interface of colluvium and highly weathered slate interlayered with sandy slate. An example of the rock quality designation (RQD) profile obtained from borehole B06 is also shown in Fig. 6. The slip surface shown in Fig. 6 is identical to that reported in a monitoring and remediation project supervised by the governmental authority (Limin Engineering Consultant 2006, 2007; Lu 2009). The slip surface locates approximately at the interface of colluviums and highly fractured (and/or weathered) slate and sandy slate strata, with RQD values distributed over a wide range. Therefore, derivations of the material properties using an undisturbed sampling technique for such a depth may be costly and time-consuming. It is well-known that several factors may influence the strength parameters to be used in the stability and/or deformation analyses for slopes. These factors include the stress-level-dependency and the strength anisotropy of the geomaterial, and the progressive failure of the slope (Huang and Tatsuoka 1994). To fully take into account these factors in a slope stability analysis requires substantial increases in work load and budget on undisturbed soil/rock sampling and laboratory testing. However, an accurate back-analysis as to be discussed here is a possible way to overcome the difficulty associated with the complexity of material strength evaluation taking into account the above factors. This is because the back-analysis finds a so-called "lumped" or "operational" material strength along the failure surface.

Figure 7(a) shows the daily rainfall recorded at a nearby weather station during the period from July, 2005 ~ May, 2006. Several peaks of daily rainfall caused by typhoons can be seen. These intensive rainfalls caused responsive groundwater table fluctuations and slope displacements, as shown in Fig. 7(b). It can also be seen that the slope displacements accumulate in a plastic manner, *i.e.*, no rebound (or decrease) of the slope displacement followed by a decreasing water table was detected. Based on Eq. (1), internal friction angle, $\phi = 32°$, is back-calculated using $c = 0$ kPa and $F_s = 1.0$ for the post-rainfall groundwater table of rainfall event No. 1 (which occurred on July 22, 2005). It is assumed in this back-calculation and also in the following analyses that the $c = 0$ kPa condition is valid for the entire slope subjected to an intensive rainfall because of the dominancy of the downward "saturation front". The condition of $c = 50$ kPa was used for the zone above the groundwater table in the pre-rainfall condition. The use of $c = 50$ kPa approximately follows a theory that the apparent cohesions increase linearly with the depth of the cover soils. It is noted that the influence on the analytical results (specifically the back-calculated ϕ and slope displacement Δ) are hardly influenced by the input values of c because both for the pre- and post-rainfall conditions, only small portions of the sliding surface are located above the groundwater table, as seen in Fig. 6.

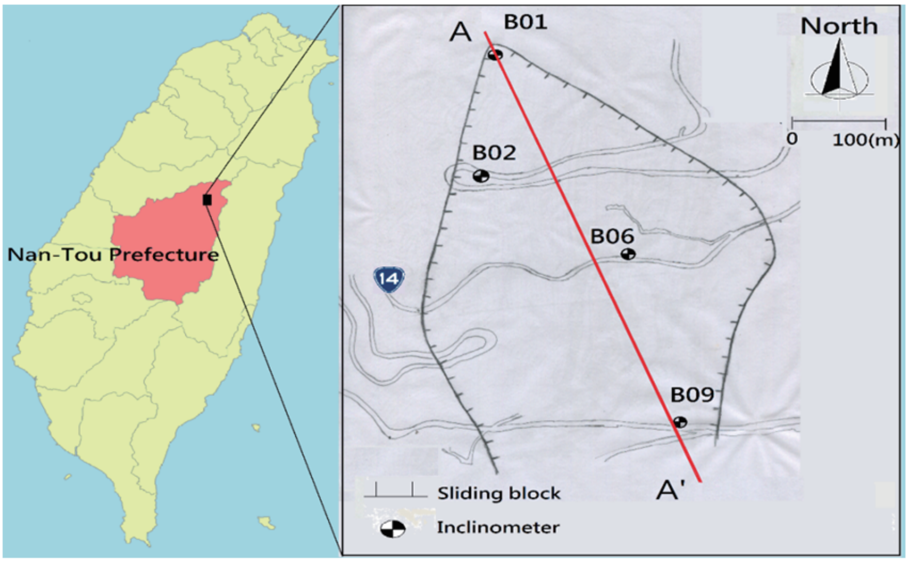

Fig. 5 Location of the Ru-San slope

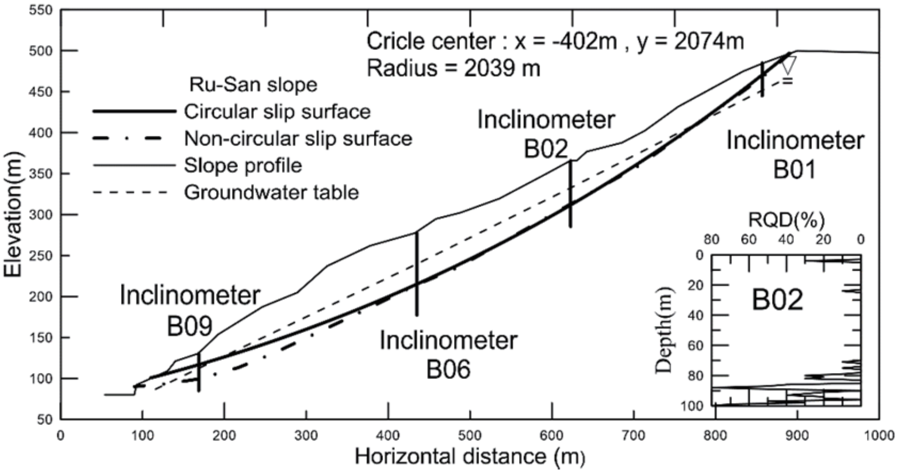

Fig. 6 Profile of the Ru-San slope

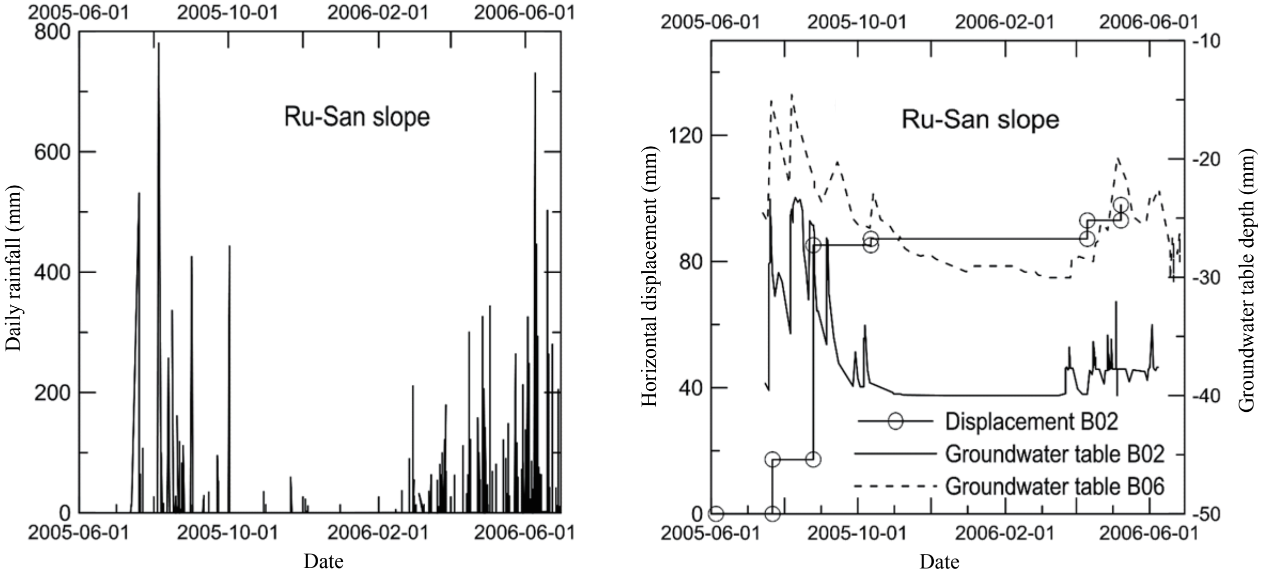

(a) Daily rainfall (b) Measured groundwater table heights and slope displacements

Fig. 7 Records of long-term monitoring for the Ru-San slope

Figure 8 shows the variation of F_s based on Eq. (1) for the failure surface subjected to the periodic groundwater table fluctuations discussed in Fig. 7(b). It can be seen that values of F_s changes between 0.90 and 1.20 in response to the fluctuation of groundwater tables during the period of monitoring. In addition, a measurable decrease of F_s occurred during the second event of rainfall (on August 25 2005) well corresponds to a significant increase of slope displacement. Due to the limitation intrinsic with the conventional slope stability analysis, the tendency in the change of F_s after the second rainfall event contradicts to that of the observed slope displacements. Figures 9(a) shows the result of a comprehensive parametric study on the incremental slope displacement induced by the groundwater table rise in the 1st event of intensive rainfall that occurred on July 22, 2005. In Fig. 9(a), only limited groups of curves ($R_f = 0.6$ and 0.9; $n = 0.05 \sim 0.4$) are shown because other groups of curves ($R_f = 0.7$ and 0.8; $n = 0.05 \sim 0.4$) fall between the two groups of curves shown. In general, the value of R_f has a more significant influence on the calculated value of Δ than that of n. Figure 9(b) shows the detail for back-calculating model parameters, K, n, R_f based on the measured slope displacement of $\Delta = 0.017$ m at X = 623.4 m (the location of inclinometer B02). In Fig. 9(b), three curves having intersections with $\Delta = 0.017$ m are shown. The parameters associated with these three curves are summarized in Table 1. In Fig. 9(b), some other curves which intersect with the line of $\Delta = 0.017$ m between the upper and lower limits of $K = 110$ and 540 are not shown for the sake of simplicity.

A comparison between the calculated and measured cumulative slope displacements is shown in Fig. 10. A maximum error of 10% ~ 40% can be found for rainfall event No. 2. For the other events under consideration, the prediction errors are marginal. The errors may stem from possible underestimations for the ground water table heights during intensive rainfalls because the measurements were performed manually after the rainfall. Therefore, the actual peak levels of the groundwater table during rainfalls may have been overlooked.

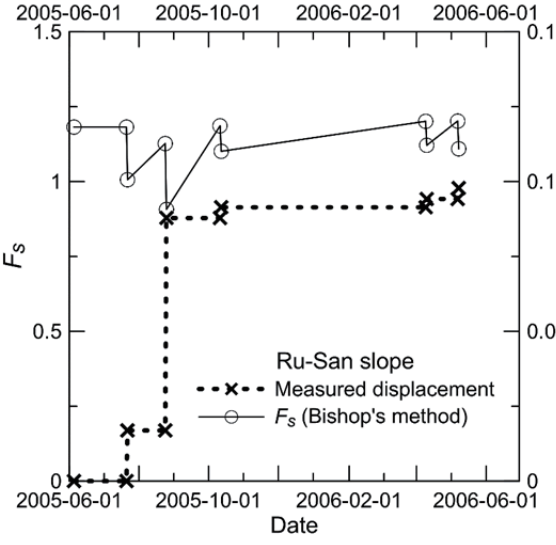

Fig. 8 Safety factors calculated using Bishop's slice methods based on the measured failure surfaces and groundwater table fluctuations

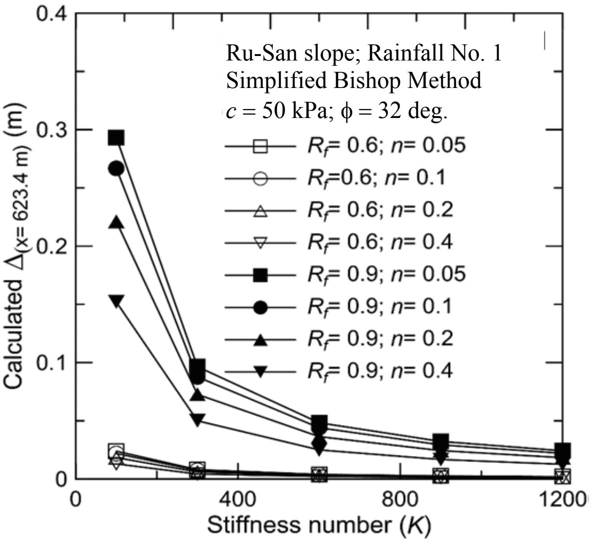

(a) General view

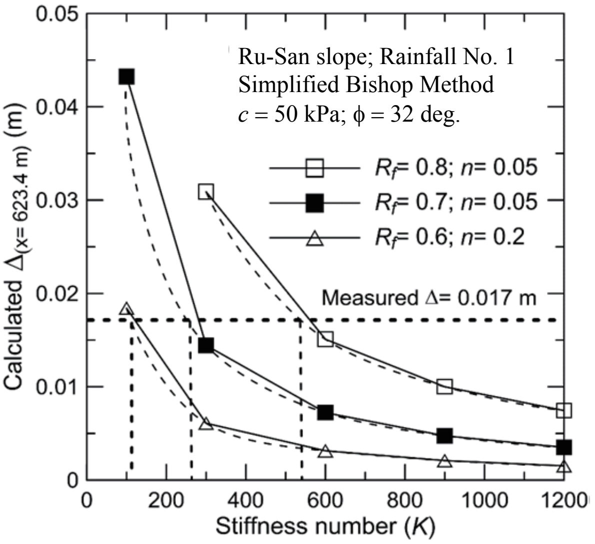

(b) Focused on the curves with $\Delta = 0.017$ m

Fig. 9 Results of parametric studies on the slope displacements using $K = 100 \sim 1200$; $n = 0.05 \sim 0.4$; $R_f = 0.6 \sim 0.9$

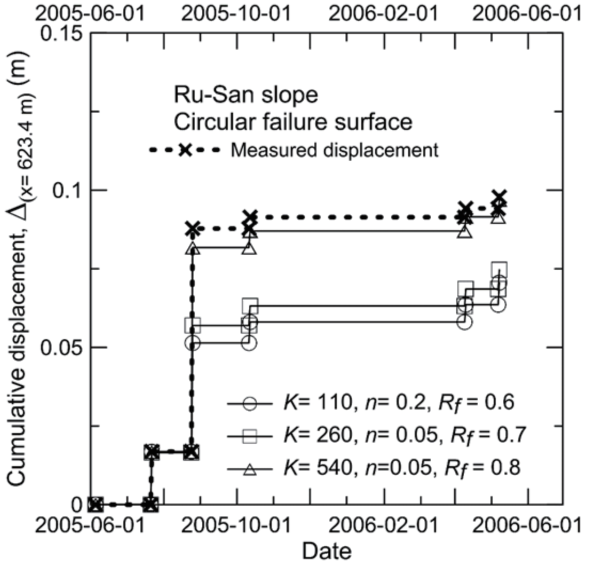

Fig. 10 Comparisons of measured and calculated cumulative slope displacements for the Ru-San slope

Table 1 Back-calculated model parameters for the Ru-San slope

No.	R_f	n	K
1	0.6	0.2	110
2	0.7	0.05	260
3	0.8	0.05	540

7. CONCLUSION

To achieve time- and cost-efficient back-calculation for the stress and deformation-related material parameters for a slope subjected to periodic rainfall-induced slope displacements, a novel procedure incorporating a conventional limit-equilibrium-based slice method and a force-equilibrium-based finite displacement method (FFDM) is proposed to back-calculate the strength and deformation-related material parameters based on the monitored data of periodic slope displacements induced by intensive rainfalls (or groundwater table fluctuations). A case history of natural slope subjected to periodic rainfall-induced displacements was used to verify the proposed approach. Soil strength and displacement-related parameters were back-calculated based on the first event of slope movement induced by a rainfall-induced groundwater table rise. These back-calculated displacement-related material parameters were then used to predict subsequent slope displacements in response to the rainfall-induced groundwater table rises. Although multiple sets of soil parameters were obtained from the back-calculation using the first event of sliding, all sets of parameters rendered acceptably accurate predictions for the subsequent events of slope sliding. The proposed procedure helps to alleviate possible difficulties associated with exploring deep-seated sliding surfaces consisting of colluviums or highly weather rocks. The present back-analysis is based on the slope displacement measured at a specific inclinometer which was the only inclinometer remained active in the long-term monitoring program. In the case of slope displacements measured at various locations of the slope, the proposed method of back-analysis is also applicable by incorporating various kinetic compatibility functions as discussed in Fig. 4. This aspect will be reported in the future.

REFERENCES

Atkinson, J.H. (1981). *Foundations and Slopes: An Introduction to Applications of Critical State Soil Mechanics*. McGraw-Hill, London.

Bishop, A.W. (1955). "The use of the slip circle in the stability analysis of slopes." *Geotechnique*, **5**, 7–17.

Fellenius, W. (1936). "Calculation of the stability of earth dams." *Proceedings of the 2nd Congress on Large Dams*, **4**, 445–463.

Ho, I.-H. (2014). "Parametric studies of slope stability analyses using three-dimensional finite element technique: Geometric effect." *Journal of GeoEngineering*, **9**(1), 33–43.

Huang, C.-C. (2013). "Developing a new slice method for slope displacement analyses." *Engineering Geology*, **157**, 39–47.

Huang, C.-C. (2014). "Force-equilibrium-based finite displacement analyses for reinforced slopes: Formulation and verification." *Geotextiles and Geomembranes*, **42**(4), 394–404.

Huang, C.-C., Hsieh, H.-Y., and Hsieh, Y.-L. (2014a). "Slope displacement analyses using force equilibrium-based finite displacement method and circular failure surface." *Journal of GeoEngineering*, **8**(3), 201–211.

Huang, C.-C., Hsieh, H.-Y., and Hsieh, Y.-L. (2014b). "Hyperbolic models for a 2-D backfill and reinforcement pullout." *Geosynthetics International*, **21**(3), 168–178.

Huang, C.-C. and Tatsuoka, F. (1994). "Stability analysis for footings on reinforced sand slopes." *Soils and Foundations*, **34**(3), 21–37.

Janbu, N. (1973). *Slope Stability Computations, Embankment-Dam Engineering*. Casagrande Volume, Hirschfeld, R.C. and Poulos, J., S.J., Eds., John Wiley & Sons, 47–86.

Lu, J.-T. (2009). *Numerical Analyses of Rainfall Induced Seepage and Movements of Lu-Shan Landslides*. Master Thesis, Department of Soil and Water Conservation, National Chung Hsing University, Taichung, Taiwan.

Limin Engineering Consultant (2006). *Report on the Landslide Investigation and Remediation Plans for 88-91 K of Route No. 14*. Soil and Water Conservation Bureau, Council of Agricultural, Executive Yuan, Taiwan (in Chinese).

Limin Engineering Consultant (2007). *Report on the Landslide Monitoring and Follow-up Restoration Plan*. The Soil and Water Conservation Bureau, Council of Agricultural, Executive Yuan, Taiwan (in Chinese).

Microsoft (2013). *Visual Studio Community 2013*.

Yeh, S.-W. (2015). *Development and Application of Hyperbolic Stress-Displacement Models*. Master Thesis, Department of Civil Engineering, National Cheng Kung University (in Chinese).